ENVIRONMENTAL RESEARCH
LETTERS

PURPOSE-LED PUBLISHING™

LETTER • OPEN ACCESS

High-resolution geophysical monitoring of moisture accumulation preceding slope movement—a path to improved early warning

To cite this article: Arnaud Watlet *et al* 2024 *Environ. Res. Lett.* **19** 124059

ENVIRONMENTAL RESEARCH
LETTERS

OPEN ACCESS

RECEIVED
18 September 2024

REVISED
1 November 2024

ACCEPTED FOR PUBLICATION
7 November 2024

PUBLISHED
19 November 2024

LETTER

High-resolution geophysical monitoring of moisture accumulation preceding slope movement—a path to improved early warning

Arnaud Watlet[1,2,*], **Paul Wilkinson**[1], **Jim Whiteley**[1,3], **Adrian White**[1], **Sebastian Uhlemann**[1,4], **Russell Swift**[1], **Susanne Ouellet**[5], **Chris Minto**[6], **Philip Meldrum**[1], **Lee Jones**[1], **David Gunn**[1], **Alastair Godfrey**[6], **Ben Dashwood**[1], **Roger Crickmore**[7], **Paul Clarkson**[6], **James Boyd**[1] and **Jonathan Chambers**[1]

[1] Shallow Geohazards and Earth Observation, British Geological Survey, Keyworth, United Kingdom
[2] Geology and Applied Geology, University of Mons, Mons, Belgium
[3] Ground Engineering & Tunnelling, AtkinsRéalis, Bristol, United Kingdom
[4] Faculty of Geosciences, University of Bremen, Bremen, Germany
[5] University of Calgary, Calgary, Canada
[6] Indeximate, Hinckley, United Kingdom
[7] Luna OptaSense, Dorchester, United Kingdom
[*] Author to whom any correspondence should be addressed.

E-mail: arnw@bgs.ac.uk

Keywords: near-surface geophysics, landslides, moisture, monitoring, natural hazards, electrical resistivity tomography, early warning

Supplementary material for this article is available online

Abstract

Slope failures are an ongoing global threat leading to significant numbers of fatalities and infrastructure damage. Landslide impact on communities can be reduced using efficient early warning systems to plan mitigation measures and protect elements at risk. This manuscript presents an innovative geophysical approach to monitoring landslide dynamics, which combines electrical resistivity tomography (ERT) and low-frequency distributed acoustic sensing (DAS), and was deployed on a slope representative of many landslides in clay rich lowland slopes. ERT is used to create detailed, dynamic moisture maps that highlight zones of moisture accumulation leading to slope instability. The link between ERT derived soil moisture and the subsequent initiation of slope deformation is confirmed by low-frequency DAS measurements, which were collocated with the ERT measurements and provide changes in strain at unprecedented spatiotemporal resolution. Auxiliary hydrological and slope displacement data support the geophysical interpretation. By revealing critical zones prone to failure, this combined ERT and DAS monitoring approach sheds new light on landslide mechanisms. This study demonstrates the advantage of including subsurface geophysical monitoring techniques to improve landslide early warning approaches, and highlights the importance of relying on observations from different sources to build effective landslide risk management strategies.

1. Introduction

Slope failures are a threat to communities around the globe. They cause significant damage to critical infrastructure and individual properties and in some cases may lead to loss of life. In recent history, landslides led to > 4500 recorded fatalities per year (Froude and Petley 2018), and billions of dollars of economic losses (Dilley 2005, Kirschbaum *et al* 2015). Even non-fatal, minor landslides may have large economic impacts as they affect critical infrastructure (Emberson *et al* 2020). These numbers are set to increase due to climate change and associated global rise in rainfall intensity, which is a major trigger of landslides (Gariano and Guzzetti 2016). While preventing landslides from occurring is impractical due to costs, the associated risks can be mitigated both at local and regional scales to reduce landslide impacts on society (Lacasse *et al* 2009). A better understanding of the morphology of unstable slopes, and the associated slope failure mechanisms is key to developing more informed risk management

strategies. Monitoring of unstable slopes, in particular, is an essential component of local landslide early warning systems (Lo-LEWS) (Maskrey 2011), which main purpose is to identify precursors of landslide events (Intrieri *et al* 2013) and locate zones that may become unstable due to changes in the subsurface conditions.

Moisture-induced landslides—also referred to as rainfall-induced landslides—are those triggered by increased soil moisture or groundwater levels, which raise pore water pressures and hence reduces effective stresses. Basic Lo-LEWS monitoring approaches mainly integrate surface displacement observations, indicating ongoing deformation but not detecting the underlying cause, which may lead to belated early warnings. Therefore, Lo-LEWS can benefit from monitoring subsurface parameters related to the driving factors of slope failure to extend the effective warning period (Lacroix *et al* 2020). Geophysics-based monitoring systems have emerged as powerful tools to track subsurface conditions of slopes prone to moisture-induced landslides (Whiteley *et al* 2019), increasing the predictive capacity of slope failure (Uhlemann *et al* 2021). Designed to non-invasively image the subsurface, and providing proxies to critical slope stability properties (e.g. moisture, suction, shear strength), geophysical methods are ideally equipped to assess the integrity of unstable slopes at various scales (Whiteley *et al* 2021a).

Electrical resistivity tomography (ERT) has long been used to investigate landslides in 2D or 3D (Jongmans and Garambois 2007), providing electrical resistivity models linked to the geology, hydrology and morphology of the landslide. More recently, time-lapse ERT (i.e. in 4D) has increasingly been applied to monitor landslides (Bièvre *et al* 2012, Lehmann *et al* 2013, Supper *et al* 2014, Gance *et al* 2016, Perrone *et al* 2014, Hojat *et al* 2019, Falae *et al* 2021, Tsai *et al* 2021, Lapenna and Perrone 2022, Wicki and Hauck 2022, Watlet *et al* 2023, Whiteley *et al* 2023). The main benefits of geoelectrical monitoring lie in the possibility to link changes in electrical resistivity to changes in subsurface conditions, mainly moisture (Slater and Binley 2021, Holmes *et al* 2022), coupled with the maturity of remote monitoring equipment specifically designed for autonomous monitoring of slope processes (Chambers *et al* 2022). At the other end of the near-surface geophysics spectrum, distributed acoustic sensing (DAS) systems have rapidly emerged as novel tools capable of detecting seismic signals (Dou *et al* 2017). More recently, DAS has shown great potential in the low-frequency domain (<1 Hz) to monitor dynamic changes in strain (Karrenbach *et al* 2019, Crickmore *et al* 2020), with promising prospect for landslide monitoring (Ouellet *et al* 2024).

While combining various geophysical methods has proven powerful for characterising landslides heterogeneity (e.g. Hibert *et al* 2012, Whiteley *et al* 2021b, Zakaria *et al* 2022), relatively few case studies have focused on integrating multiple complementary geophysical techniques for monitoring and predicting landslide processes. Most geophysical monitoring applications focus on a primary technique, potentially supplemented with additional methods at varying scales, such as geotechnical or remote sensing data (e.g. Jaboyedoff *et al* 2019, Thirugnanam *et al* 2022), which together provide critical insights into subsurface conditions impacting slope stability. Yet, differences in the scales of these data sources can complicate direct correlations between subsurface measurements and surface deformation, thereby limiting early warning capabilities.

Hence, can we elucidate the relationship between locally elevated soil moisture and slope deformation by integrating high-resolution ERT imaging with spatially distributed deformation sensing? We present, to the best of our knowledge, the first 4D ERT imaging of slope movement supported by strain measurements from low-frequency DAS at comparable scales, and hydrological and geotechnical datasets. With this study, we aim to demonstrate the advanced capability to detect precursory conditions to slope displacement. Incorporating 4D soil moisture data in the feed of information used to assess slope stability has the potential to improve landslide early warning strategies, thereby enhancing landslide risk mitigation.

2. Site description and methodology

2.1. The hollin hill landslide observatory (HHLO)

The HHLO (figure 1, Chambers *et al* 2011, Gunn *et al* 2013) in North Yorkshire, UK, was designed in the mid-2000s as a test site for developing novel geophysical monitoring of unstable slopes. The site features a moisture-induced, slow-moving landslide, representative of many clay-rich lowland landslides worldwide. It has a well-documented history of seasonal reactivation with peaks in movement generally occurring during winter, between December and March (see figure S1 in the supplementary material) due to reduced evapotranspiration. The landslide's morphology largely depends on the underlying geological structure. The south-facing slope comprises two main geological units (Lower to Late Jurassic) gently dipping to the North: the Whitby Mudstone Formation (WMF) and the Staithes Sandstone Formation (SSF). Due to lower permeability and high plasticity, the WMF slowly creeps over the SSF when reaching elevated moisture contents. This translational movement mostly occurs in the central part of the slope. In the

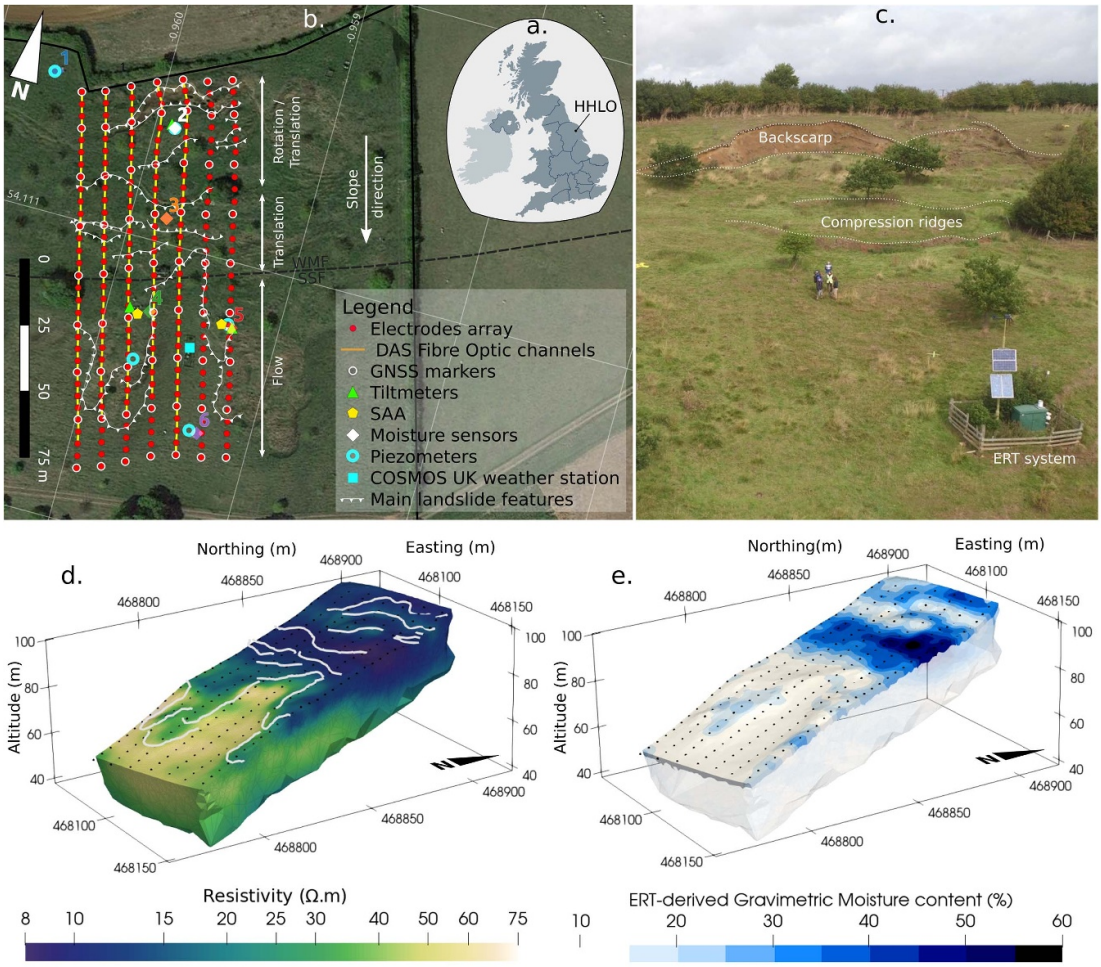

Figure 1. (a) Location of Hollin Hill on UK map, (b) map of the HHLO displaying the location of the ERT array, fibre optic cable, point sensors (and location number), GNSS markers and main landslide features; (c) drone photo highlighting the backscarp and compression ridges of the HHLO. (d) Resistivity model and (e) ERT-derived GMC model for the monitoring baseline (22 November 2020).

top part, a complex rotational failure within the WMF is observed, linked to the mass wasting generated by creeping downslope (Uhlemann *et al* 2017, Boyd *et al* 2021). The hydrogeological context of the HHLO includes the occurrence of perched water tables at shallow depth (Gunn *et al* 2013) overlying a deeper regional groundwater table.

Since first deployed in 2008, 4D geoelectrical imaging revealed complex, seasonal moisture dynamics in the slope (Uhlemann *et al* 2017, Merritt *et al* 2018). Preferential infiltration and moisture build-up have also been linked with periods of increased movements, and evidence of superficial drying processes are associated with surface shrinking and cracking. However, properly demonstrating that local zones of elevated moisture content were leading to co-located displacement or slope failure has been challenging. One main reason has been the challenge of monitoring slope deformation at a spatial and temporal scale comparable to that of time-lapse ERT measurements (Kelevitz *et al* 2022). Deriving electrode movements from time-lapse ERT measurements was successfully developed (Wilkinson *et al* 2015, 2016), providing a means of tracking large displacements greater than 10% of the electrode spacing. But other techniques providing independent measurement of surface deformation at higher resolution, such as strain from low-frequency DAS, ideally complement the toolbox of monitoring techniques able to detect minor movements precursory to larger slope failure.

Over the years, state-of-the-art sensors have also been deployed at the HHLO to provide independent measurements for comparison and interpretation alongside geophysics-based monitoring. Clusters of point sensors including shallow soil moisture (at 20 cm and 50 cm bgl), matric potential (at 50 cm bgl) and piezometers monitoring water level in shallow and deep boreholes are distributed over 6 locations (1–6 in figure 1). Ground deformation associated with the landslide activity is also tracked via four independent approaches at the HHLO, including tiltmeters (at location 2, 4 and 5), Shape Accelerometers Arrays (SAA; Abdoun *et al* 2013) (at location 4 and 5), GNSS marker pegs and repeated LiDAR scans (see table S1 and text S3 in the supplementary material for more details; Lague *et al* 2013)

2.2. Gravimetric water content from electrical resistivity tomography

The PRIME system installed since November 2020 at the HHLO is a low-cost and low-power ERT instrument designed for remotely monitoring slope condition (Holmes *et al* 2020). ERT measurements are acquired on a scheduled, daily basis and telemetered to remote servers through 4G internet. The ERT array comprises seven lines oriented in the slope direction, each with 32 electrodes, forming a grid of 224 electrodes with a separation of 9.5 m across the slope and 4.75 m along the slope (see figure 1). A comparable ERT array layout was installed for a decade (2008–2019) at the HHLO (Kuras *et al* 2009), and proved to capture shallow hydrological processes throughout the hillslope (Uhlemann *et al* 2017, Merritt *et al* 2018). ERT time-lapse inversion follows a hybrid inversion scheme mimicking a time-lapse inversion but incorporating potential electrode movements as monitored by repeated GNSS surveys of a network of ground control points (Uhlemann *et al* 2016, Boyd *et al* 2021). Since only one large slope displacement event occurred within the time window presented in this manuscript (22 November 2020–30 March 2022), electrode locations have been adapted only once following this event. Adjusted electrode locations are derived from inverting the ERT data for electrode movements, following a methodology developed in (Wilkinson *et al* 2015, 2016).

In this study, we present ERT monitoring results as soil moisture models. Resistivity models are translated into gravimetric moisture content (GMC) models after inversion and temperature correction, following the approach by Uhlemann *et al* (2017), calibrated for the HHLO by Merritt *et al* (2016) using Waxman and Smits (1968) relationships (figures 1(d) and (e)). The calibration was performed on soil and shallow borehole core samples from the SSF and WMF. We use separate parameter sets for the WMF and the SSF as in Uhlemann *et al* (2017). Boyd *et al* (2024) has highlighted that this relationship is likely to be valid only at shallow depths, given that Waxman-Smits equation parameters change for deeper, more consolidated rocks. Therefore, the GMC models are generated using the relationship developed by Uhlemann *et al* (2017) applied to the first 2 m below the ground surface, which represents the layer above mapped shear zones. However, due to the presence of perched water levels at ∼2 m below ground level (bgl), especially in the WMF, most temporal changes in resistivity, and therefore GMC, are expected to occur at shallow depth. More detailed on the acquisition processing and correction of the ERT data is available in text S1 of the supplementary materials (Keller and Frischknecht 1966, Brunet *et al* 2010, Mwakanyamale *et al* 2012). Text S1 also contains information on the spatial resolution of the resistivity models.

2.3. Strain from low-frequency distributed acoustic sensing

We rely on strain measurements acquired by a DAS system along a fibre optic cable deployed at the HHLO (Clarkson *et al* 2021). The DAS system consists of a Luna Optasense ODH-F interrogator unit which transmits coherent laser pulses within the fibre, and acts as a distributed interferometer. Any strain disturbance to the fibre changes the optical phase of the backscattered light (Bao and Chen 2012, Bao and Wang 2021) and can be recorded. A low-pass filter at 1 Hz is applied to the DAS data and optical phase data are converted to units of strain. The fibre was buried at ∼10 cm bgl within narrow trenches along the slope direction to form six lines, five of which are co-located with the easternmost five lines of the ERT array. The strain measurements derived from low-frequency DAS are sampled with a 1 m spatial interval over a gauge length of 4 m, which defines the spatial resolution (detailed processing, including temperature correction, in text S2 of the supplementary material). In this study, we investigate change in strain averaged at daily time intervals on two periods overlapping the ERT dataset from 22 November 2020 to 30 January 2021 (70 d), and then from 22 November 2021 to 28 February 2022 (100 d), each focusing on the wettest part of the season. Data are expressed as cumulative change in microstrain ($\mu\varepsilon$) with respect to a baseline set at the beginning of each period.

3. Results and discussion

3.1. Moisture accumulation preceding landslide reactivation

The ERT-derived soil moisture dataset of this study starts on 22 November 2020. Increase in GMC is displayed at regular intervals before the main slope displacement event on 20–21 January 2021 (figure 2). This increase is most pronounced in the WMF formation, especially above the backscarp and in the area of the rotational slip, with localised increases higher than 10% GMC. This general moisture trend is corroborated by the network of soil moisture sensors. The backscarp itself stays relatively dry, contrasting with the zone directly above and below. The steepness of the scarp combined with locally lower permeability near the slip plane favors surface run-off processes, hindering in-situ water infiltration. The resistivity models in the backscarp region also show preferential flow between the zone above the scarp and the flatter region at the toe of the scarp, favoring moisture accumulation (see figure S2 in the supplementary material).

Deformation data show that the 2021 reactivation started with two minor precursory displacement events (in the order of 1 mm recorded by the shallowest SAA at 10 cm bgl) following rainfall events, on 27 December 2020 and 14 January 2021 (figure 3). The

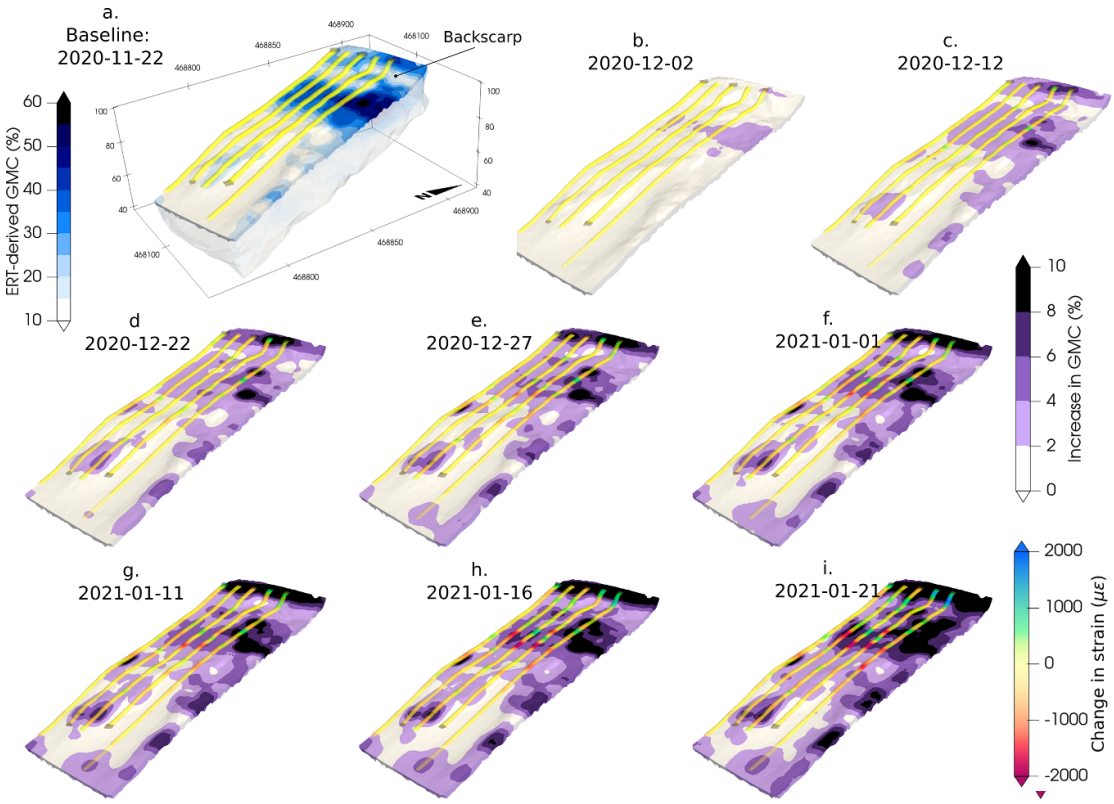

Figure 2. ERT-derived gravimetric moisture content (GMC) model for the baseline on 22 November 2020 (a), and models of relative increase in GMC with respect to the baseline displayed on a selection of time-steps (b)–(i). Recorded changes in microstrain are also shown. See animated version in the supplementary materials.

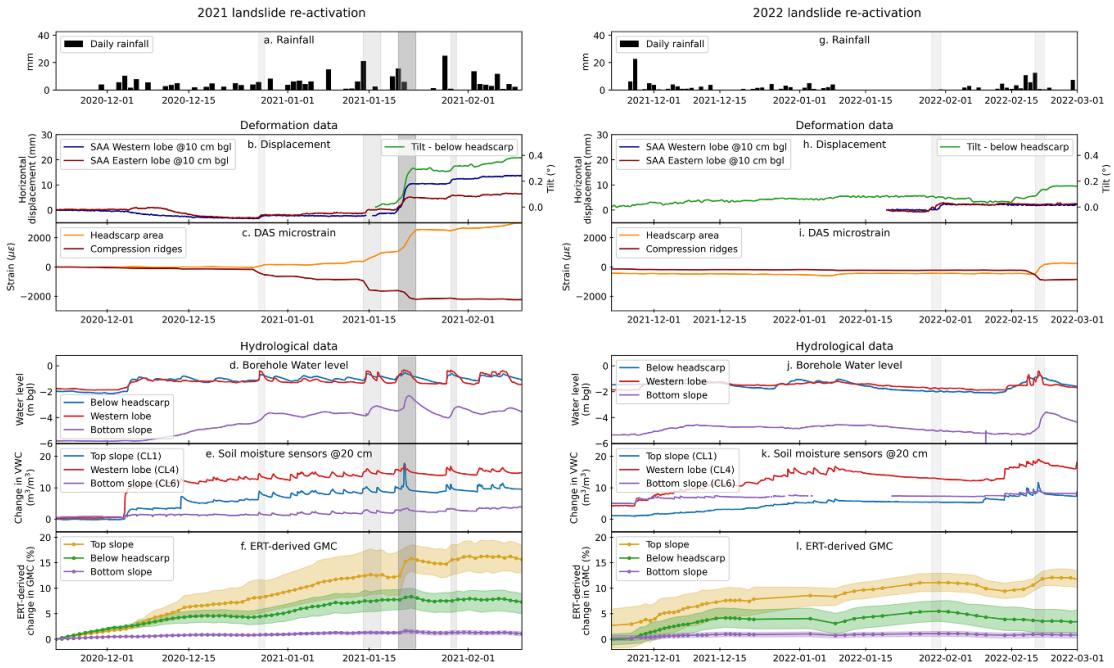

Figure 3. Summary of the geophysical, hydrological and displacement datasets acquired during the 2021 (a)–(f) and 2022 (g)–(l) landslide reactivation periods (November 2020 to February 2021, and November 2021 to March 2022). Figures display rainfall (a), (g), surface displacement (b), (h), DAS microstrain (c), (i) using channels highlighted in figure S3, borehole water level (d), (j), soil moisture at 20 cm bgl (e), (k), ERT-derived GMC (f), (l). Grey boxes indicate periods of minor (light grey) and major (dark grey) deformation event.

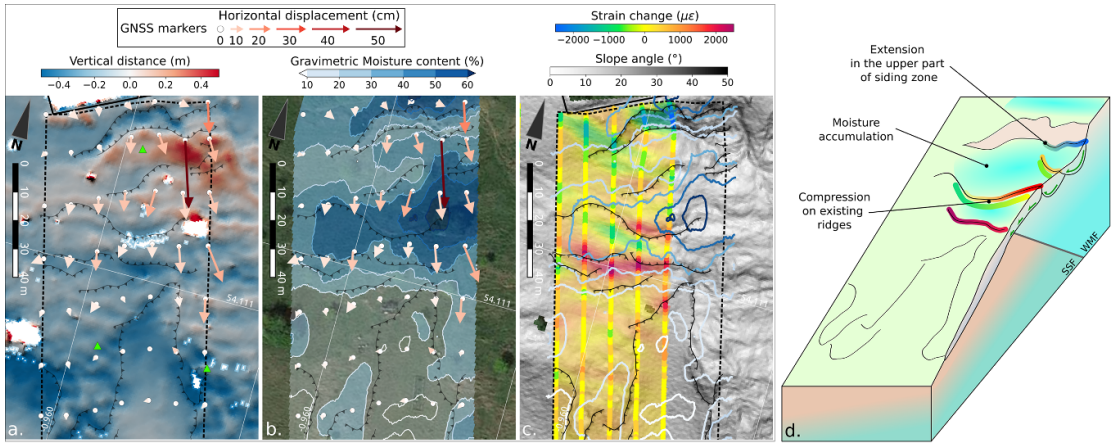

Figure 4. Maps showing (a) vertical displacement computed from LiDAR scans from November 2020 and September 2021, and horizontal displacement on the network of GNSS markers between 15 January 2021 and 20 February 2021; (b) ERT-derived GMC following peak movement in landslide reactivation 2021 (22 January 2021) as compared to GNSS markers displacement; (c) strain change recorded on the fibre and interpolated, and compared to GMC contour lines following peak movement (22 January 2021); (d) sketch describing the landside dynamics at the HHLO and the geophysical observations on the ERT and DAS monitoring systems.

first precursor event seems to have predominantly affected the middle part of the slope, where change in microstrain indicates compression in the mid-slope ridges (figure 4). The second precursory event followed snowfall and a three-day time window is documented using strain data from the low-frequency DAS at 1 min sampling frequency in Ouellet *et al* (2024). It started with mid-slope deformation, then propagated upslope to the backscarp. The main deformation occurred on 20–21 January 2021, as Storm Christophe hit the UK. Deformation was mainly confined to the top part of the slope underneath the backscarp, as corroborated by the microstrain data (figure 3(c)), with two main transverse zones of compressions on existing ridges, and extension in the backscarp. The top-slope tiltmeter recorded a tilt step of 0.3° in the slope direction, indicating rotational processes. The mid-slope tiltmeters showed no change, although the western SAA recorded ∼12 mm horizontal displacement, indicating minor translational movement mid-slope (figure 3(b)). Following this main event, two minor events were visible in the tiltmeters and SAA data on 29 January 2021 and 19 February 2021, with respectively 2 mm and 1 mm as recorded by the SAA, as well as 0.04° and 0.02° recorded by the top-slope tiltmeter.

In 2022, the landslide remained comparatively stable, with only a few minor deformation events. Each observed deformation in 2022 is visible in only one of the datasets from DAS (figure 3(i)), SAA, or the top-slope tilt-meter (figure 3(h)), indicating much smaller and more localized deformation than in 2021. This is confirmed by the GNSS surveys and LIDAR scans which detected no noticeable surface topography variation.

3.2. Landslide mechanism

A joint analysis of vertical displacement (from LIDAR surveys), horizontal displacement (from GNSS markers), tilt data and downslope strain (from low-frequency DAS) during the 20–21 January event highlights rotational movement mainly in a small area underneath the backscarp, where ground elevation increased below a zone of extension on the fiber. This area coincides with the GNSS marker with the highest horizontal displacement, confirming a combination of translational and rotational movement, limited to the top half of the slope. Despite a lack of temporal resolution in the geophysics-based data, comparing tilt change at the top of the slope and displacement data from the central slope SAA suggests similar dynamics as described by Ouellet *et al* (2024), with central slope destabilization and horizontal displacement propagating and amplifying upslope, including a rotational component when reaching the backscarp zone. During the 14 January precursory event, high temporal resolution low-frequency DAS (Ouellet *et al* 2024) showed that this retrogressional behavior propagated from the central slope to the backscarp at ∼1.7 m h^{-1}. Similar retrogressive dynamics were also identified at larger timescales by large mobilization of the flow lobes in 2013 followed by the development of the backscarp in 2016.

The top-slope tiltmeter showed significant downslope tilt starting on 20 January 2021 around 20:00 UTC, peaking between 02:00 and 03.00 UTC on 21 January 2021, coinciding with a peak in moisture content at the top of the slope. Peak displacement lasted 15 h, as inferred from the tilt data. This event cannot be related to a particularly extreme rainfall event, with only 10 and 15.6 mm on 19 and 20

January. Rainfall on 20 January was low but sustained, becoming more intense towards the evening with 9.59 mm recorded over 4 h starting from 20:00, peaking at 22:00. Despite the daily rainfall being unremarkable, this 4 h event was the most intense since summer 2020 and the second highest over winter 2021, linked to smaller movements recorded by the SAA and tiltmeters.

However, the main deformation event and precursors occurred in the area with the highest moisture content (>40% GMC and up to 55% GMC) as established by the ERT monitoring, and the highest increase in moisture with respect to the baseline (>10% GMC, figure 2). This confirms elevated soil moisture as the driving factor for ground displacement, with WMF mudstone material potentially reaching a local liquid limit. GMC higher than 55% matches with liquid limits previously measured on WMF soil samples (Merritt *et al* 2014) and fits well with previously obtained thresholds for landslide activation of 49% (Uhlemann *et al* 2017). Data from moisture sensors and piezometers show high peaks in moisture and water level starting at 22:00, which are hard to explain solely by local rainfall. As a consequence of Storm Christophe hitting the UK, heavy rain with spatially varying intensity was recorded in Northern England (Met Office 2021). It is likely that the event was triggered by surface or subsurface run-off from that plateau upslope, temporarily saturating parts of the hillslope already at high moisture levels. Rain rate data from NIMROD MET-Office rainfall radar (over 1 km^2 cells and 5 min intervals; (Met Office 2003)) reveals that more intense rainfall occurred just north of the site, on the plateau directly upslope of the hill.

3.3. Combining ERT and low-frequency DAS and implications for landslide early warning

This study highlights the complementarity of ERT and low-frequency DAS to reveal the mechanisms leading to slope deformation with unprecedented detail. The ERT-based moisture imaging provides time-lapse snapshots of the subsurface with high spatial resolution, setting the moisture condition context throughout the slope. Despite the 3D ERT-based GMC models being displayed on a relatively fine mesh, the overall resolution depends on the electrode separation, which is relatively sparse at the HHLO (see section 2). As discussed in Uhlemann *et al* (2017), this layout has the benefit of sampling a large portion of the hillslope, while limiting the capability of the system to image subtle shallow resistivity changes but providing spatially continuous images at depths closer to the expected slip surface. This is precisely where the complementarity with the low-frequency DAS is most powerful. By providing strain data at shallow depth (∼10 cm), with high spatial resolution along the FO cable, i.e. in the slope direction, it provides direct and localised information on slope stability in the near surface where the ERT system has poor sensitivity.

The ERT-derived moisture models accurately delineate zones of interest (figure 4(d)) where moisture slowly builds up, and the WMF clay materials are above the plastic limit, locally reaching the liquid limit. Slope deformation occurred in an area that showed elevated moisture contents in the weeks prior to movement. The low-frequency DAS complements these observations by identifying strain changes at the edge of the zones of elevated moisture, as minor displacement occurs. This demonstrates that calibrated time-lapse ERT providing spatio-temporal soil moisture dynamics, effectively validates elevated soil moisture as the cause of slope movement, and identifies zones where landslide susceptibility increases. DAS strain data then sheds light on how the elevated moisture translates in terms of slope stability. Crucially, the co-location of these measurements allows time-lapse imaging of holistic slope processes that cannot be practicably replicated using point sensors nor rainfall data alone. This makes it extremely valuable for both sources of geophysical information to jointly feed a new generation of Lo-LEWS looking at changes in co-related material properties (Bogaard and Greco 2018, Segoni *et al* 2018, Whiteley *et al* 2021a), with a particular interest in the surveillance of critical infrastructures, such as long linear assets (e.g. railway cutting, flood embankment, etc.).

Datasets acquired at the HHLO prior to the relatively minor slope deformation event in 2021 also help to improve the definition of thresholds that can be used to issue Lo-LEWS alarms for future, potentially larger events. For instance, no significant movement was recorded in 2022. Comparing the ERT-derived moisture models from January 2021 and during winter 2022 shows that moisture was at lower levels throughout the slope, particularly in the top of the slope where zones with the highest moisture contents remained below the thresholds of the January 2021 event (figures 3(f) and (l)).

4. Summary

This study presents the deployment of a long-term ERT and strain monitoring from low frequency DAS at the Hollin Hill Landslide Observatory (HHLO), together with a network of hydrological and geotechnical sensors and techniques. It represents, to the best of our knowledge, the first combination of ERT and DAS monitoring on an active slow-moving landslide. Through a robust and already well documented methodology, daily 3D electrical resistivity models are transformed into shallow soil moisture models at high spatial resolution. These reveals zones of moisture accumulation in the top part of the slope, which eventually led to slope movement, with a peak in January 2021, as revealed with an unprecedented spatial resolution by changes in strain measured by

the low-frequency DAS along a fibre optic cable co-located with the ERT array.

Results from this interdisciplinary approach highlight the efficacy of integrating multiple geophysical methods together to enhance the observability and understanding of landslide mechanisms. A notable strength of this approach lies in the capability of ERT, via high-spatial resolution imaging, to delineate zones of elevated moisture content, which can be interpreted as precursory indicators of slope instability. Unlike point sensors, which do not provide spatially continuous measurements of subsurface properties, the ERT and DAS monitoring capability described in this study can provide high-resolution spatiotemporal images that allow a holistic assessment of subsurface processes at the whole-slope scale. Building up on this study, future applications should aim to further integrate the outputs of both ERT and DAS monitoring within early warning systems. Given that both methods have proven highly complementary, this study also calls for similar experiments to be conducted in analogous environments, such as for monitoring ground subsidence, volcanic uplift or shallow degassing processes, as well as CO_2 storage-related activities. Overall, this study offers novel ways to address the critical need to advance the observational capability in slope stability analysis, which will inevitably lead to improved early warning systems and to better informed risk management strategies, and therefore enhance the resilience of societies to landslide hazards worldwide.

Data availability statement

The data that support the findings of this study are openly available at the following URL/DOI: https://zenodo.org/records/13118624.

Acknowledgment

BGS authors publish with the permission of the Executive Director, British Geological Survey (UKRI-NERC). We would like to thank Josie Gibson, Frances Standen and James Standen for their continued support at Hollin Hill. We also thank Brendon Purnell from Luna Optasense, and members of Environmental & Engineering Geophysics at BGS, including Mihai Cimpoiasu, Harry Harrison, Jessica Holmes, Cornelia Inauen, Oliver Kuras and Dave Morgan for their help and support. Processed data from ERT, low-frequency DAS, soil moisture sensors, tilt-meters, Shape Accelerometer Arrrays, LiDAR scans, GNSS surveys are available at Zenodo via https://doi.org/10.5281/zenodo.13118623 with Creative Commons Attribution 4.0 International license (British Geological Survey 2024). ERT data were pre-processed using Pandas (McKinney *et al* 2010), and Resipy (Blanchy *et al* 2020; https://resipy.org), inversions were performed using E4D (Johnson *et al* 2010; www.pnnl.gov/projects/e4d). Figures were created using Matplotlib (Hunter *et al* 2007); Paraview (Ahrens *et al* 2005), Qgis and InkScape. We thank two anonymous referees and the handling editor for their thoughtful comment which have contributed to improve this study.

ORCID iDs

Arnaud Watlet https://orcid.org/0000-0003-0318-9032
Jim Whiteley https://orcid.org/0000-0001-5254-4817
Sebastian Uhlemann https://orcid.org/0000-0002-7673-7346
Russell Swift https://orcid.org/0000-0002-4739-9587
Ben Dashwood https://orcid.org/0000-0002-8396-861X
James Boyd https://orcid.org/0000-0002-3748-8535
Jonathan Chambers https://orcid.org/0000-0002-8135-776X

References

Abdoun T, Bennett V, Desrosiers T, Simm J and Barendse M 2013 Asset management and safety assessment of levees and earthen dams through comprehensive real-time field monitoring *Geotechnol. Geol. Eng.* **31** 833–43

Ahrens J, Geveci B, Law C, Hansen C and Johnson C 2005 Paraview: an end-user tool for large-data visualization *The Visualization Handbook* vol 717 (Elsevier) pp 50038–1

Bao X and Chen L 2012 Recent progress in distributed fiber optic sensors *Sensors* **12** 8601–39

Bao X and Wang Y 2021 Recent advancements in rayleigh scattering-based distributed fiber sensors *Adv. Devices Instrum.* **2021** 8696571

Bièvre G, Jongmans D, Winiarski T and Zumbo V 2012 Application of geophysical measurements for assessing the role of fissures in water infiltration within a clay landslide (Trièves area, French Alps) *Hydrol. Process.* **26** 2128–42

Blanchy G, Saneiyan S, Boyd J, McLachlan P and Binley A 2020 ResIPy, an intuitive open source software for complex geoelectrical inversion/modeling *Comput. Geosci.* **137** 104423

Bogaard T and Greco R 2018 Invited perspectives: hydrological perspectives on precipitation intensity-duration thresholds for landslide initiation: proposing hydro-meteorological thresholds *Nat. Hazards Earth Syst. Sci.* **18** 31–39

Boyd J P, Binley A, Wilkinson P, Holmes J, Bruce E and Chambers J 2024 Practical considerations for using petrophysics and geoelectrical methods on clay rich landslides *Eng. Geol.* **334** 107506

Boyd J *et al* 2021 A linked geomorphological and geophysical modelling methodology applied to an active landslide *Landslides* (Springer) pp 1–16

British Geological Survey 2024 Data used in manuscript "High-resolution geophysical monitoring of moisture accumulation preceding slope movement—a path to improved early warning" (https://doi.org/10.5281/zenodo.1311862)

Brunet P, Clément R and Bouvier C 2010 Monitoring soil water content and deficit using electrical resistivity tomography (ERT)—a case study in the Cevennes area, France *J. Hydrol.* **380** 146–53

Chambers J E et al 2011 Three-dimensional geophysical anatomy of an active landslide in Lias Group mudrocks, Cleveland Basin, UK *Geomorphology* **125** 472–84
Chambers J et al 2022 Long-term geoelectrical monitoring of landslides in natural and engineered slopes *Lead. Edge* **41** 768–76
Clarkson P et al 2021 Ground condition monitoring of a landslide using distributed rayleigh sensing *EAGE GeoTech 2021 Second EAGE Workshop on Distributed Fibre Optic Sensing* vol 2021 (European Association of Geoscientists & Engineers) pp 1–5
Crickmore R, Godfrey A and Minto C 2020 Temperature and strain separation from a distributed rayleigh system *EAGE Workshop on Fiber Optic Sensing for Energy Applications in Asia Pacific* vol 2020 (European Association of Geoscientists & Engineers) pp 1–4
Dilley M 2005 *Natural Disaster Hotspots: A Global Risk Analysis* vol 5 (World Bank Publications)
Dou S, Lindsey N, Wagner A M, Daley T M, Freifeld B, Robertson M, Peterson J, Ulrich C, Martin E R and Ajo-Franklin J B 2017 Distributed acoustic sensing for seismic monitoring of the near surface: a traffic-noise interferometry case study *Sci. Rep.* **7** 1–12
Emberson R, Kirschbaum D and Stanley T 2020 New global characterization of landslide exposure *Nat. Hazards Earth Syst. Sci. Discuss.* **2020** 1–21
Falae P O, Dash R K, Kanungo D P and Chauhan P K S 2021 Interpretation on water seepage and degree of weathering in a landslide based on pre-and post-monsoon electrical resistivity tomography *Near Surf. Geophys.* **19** 315–33
Froude M J and Petley D N 2018 Global fatal landslide occurrence from 2004 to 2016 *Nat. Hazards Earth Sys. Sci.* **18** 2161–81
Gance J, Malet J-P, Supper R, Sailhac P, Ottowitz D and Jochum B 2016 Permanent electrical resistivity measurements for monitoring water circulation in clayey landslides *J. Appl. Geophys.* **126** 98–115
Gariano S L and Guzzetti F 2016 Landslides in a changing climate *Earth Sci. Rev.* **162** 227–52
Gunn D A, Chambers J E, Hobbs P R N, Ford J R, Wilkinson P B, Jenkins G O and Merritt A 2013 Rapid observations to guide the design of systems for long-term monitoring of a complex landslide in the Upper Lias clays of North Yorkshire, UK *Q. J. Eng. Geol. Hydrogeol.* **46** 323–36
Hibert C, Grandjean G, Bitri A, Travelletti J and Malet J P 2012 Characterizing landslides through geophysical data fusion: example of the La Valette landslide (France) *Eng. Geol.* **128** 23–29
Hojat A, Arosio D, Ivanov V I, Longoni L, Papini M, Scaioni M, Tresoldi G and Zanzi L 2019 Geoelectrical characterization and monitoring of slopes on a rainfall-triggered landslide simulator *J. Appl. Geophys.* **170** 103844
Holmes J et al 2020 Four-dimensional electrical resistivity tomography for continuous, near-real-time monitoring of a landslide affecting transport infrastructure in British Columbia, Canada *Near Surface Geophysics* Wiley Online Library
Holmes J et al 2022 Application of petrophysical relationships to electrical resistivity models for assessing the stability of a landslide in British Columbia, Canada *Eng. Geol.* **301** 106613
Hunter J D 2007 Matplotlib: a 2D graphics environment *Comput. Sci. Eng.* **9** 90–95
Intrieri E, Gigli G, Casagli N and Nadim F 2013 Brief communication" landslide early warning system: toolbox and general concepts *Nat. Hazards Earth Sys. Sci.* **13** 85–90
Jaboyedoff M, Del Gaudio V, Derron M H, Grandjean G and Jongmans D 2019 Characterizing and monitoring landslide processes using remote sensing and geophysics *Eng. Geol.* **259** 105167
Johnson T C, Versteeg R J, Ward A, Day-Lewis F D and Revil A 2010 Improved hydrogeophysical characterization and monitoring through high performance electrical geophysical modeling and inversion *Geophysics* **75** WA27–41
Jongmans D and Garambois S 2007 Geophysical investigation of landslides: a review *Bull. Soc. Géol. France* **178** 101–12
Karrenbach M, Cole S, Ridge A, Boone K, Kahn D, Rich J, Silver K and Langton D 2019 Fiber-optic distributed acoustic sensing of microseismicity, strain and temperature during hydraulic fracturing *Geophysics* **84** D11–D23
Kelevitz K, Novellino A, Watlet A, Boyd J, Whiteley J, Chambers J, Jordan C, Wright T, Hooper A and Biggs J 2022 Ground and satellite-based methods of measuring deformation at a UK landslide observatory: comparison and integration Remote Sens. **14** 2836
Keller G V and Frischknecht F C 1966 Electrical methods in geophysical prospecting
Kirschbaum D, Stanley T and Zhou Y 2015 Spatial and temporal analysis of a global landslide catalog *Geomorphology* **249** 4–15
Kuras O, Pritchard J D, Meldrum P I, Chambers J E, Wilkinson P B, Ogilvy R D and Wealthall G P 2009 Monitoring hydraulic processes with automated time-lapse electrical resistivity tomography (ALERT) *C.R. Geosci.* **341** 868–85
Lacasse S, Nadim F, Lacasse S and Nadim F 2009 Landslide risk assessment and mitigation strategy *Landslides—Disaster Risk Reduction* ed K Sassa and P Canuti (Springer) pp 31–61
Lacroix P, Handwerger A L and Bièvre G 2020 Life and death of slow-moving landslides *Nat. Rev. Earth Environ.* **1** 404–19
Lague D, Brodu N and Leroux J 2013 Accurate 3D comparison of complex topography with terrestrial laser scanner: application to the Rangitikei canyon (N-Z) *ISPRS J. Photogramm. Remote Sens.* **82** 10–26
Lapenna V and Perrone A 2022 Time-lapse electrical resistivity tomography (TL-ERT) for landslide monitoring: recent advances and future directions *Appl. Sci.* **12** 1425
Lehmann P, Gambazzi F, Suski B, Baron L, Askarinejad A, Springman S M, Holliger K and Or D 2013 Evolution of soil wetting patterns preceding a hydrologically induced landslide inferred from electrical resistivity survey and point measurements of volumetric water content and pore water pressure *Water Resour. Res.* **49** 7992–8004
Maskrey A 2011 Revisiting community-based disaster risk management *Environ. Hazards* **10** 42–52
McKinney W, van der Walt S and Millman J 2010 *Proc. 9th Python in Science Conf.*
Merritt A J, Chambers J E, Murphy W, Wilkinson P B, West L J, Gunn D A, Meldrum P I, Kirkham M and Dixon N 2014 3D ground model development for an active landslide in Lias mudrocks using geophysical, remote sensing and geotechnical methods *Landslides* **11** 537–50
Merritt A J, Chambers J E, Murphy W, Wilkinson P B, West L J, Uhlemann S, Meldrum P I and Gunn D 2018 Landslide activation behaviour illuminated by electrical resistance monitoring: landslide activation behaviour *Earth Surf. Process. Landf.* **43** 1321–34
Merritt A J, Chambers J E, Wilkinson P B, West L J, Murphy W, Gunn D and Uhlemann S 2016 Measurement and modelling of moisture—electrical resistivity relationship of fine-grained unsaturated soils and electrical anisotropy *J. Appl. Geophys.* **124** 155–65
Met Office 2003 1 km resolution UK composite rainfall data from the met office nimrod system (NCAS British Atmospheric Data Centre) (available at: https://catalogue.ceda.ac.uk/uuid/27dd6ffba67f667a18c62de5c3456350)
Met Office 2021 Daily weather summary 2021 (available at: https://digital.nmla.metoffice.gov.uk/IO_e9deeb04-8105-4f31-94d6-7d94c00b3c21/)
Mwakanyamale K, Slater L, Binley A and Ntarlagiannis D 2012 Lithologic imaging using complex conductivity: lessons learned from the Hanford 300 Area *Geophysics* **77** E397–09
Ouellet S M, Dettmer J, Lato M J, Cole S, Hutchinson D J, Karrenbach M, Dashwood B, Chambers J E and Crickmore R 2024 Previously hidden landslide processes revealed using distributed acoustic sensing with nanostrain-rate sensitivity *Nat. Commun.* **15** 6239

Perrone A, Lapenna V and Piscitelli S 2014 Electrical resistivity tomography technique for landslide investigation: a review *Earth Sci. Rev.* **135** 65–82

Segoni S, Piciullo L and Gariano S L 2018 A review of the recent literature on rainfall thresholds for landslide occurrence *Landslides* **15** 1483–501

Slater L and Binley A 2021 Advancing hydrological process understanding from long-term resistivity monitoring systems *Wiley Interdiscip. Rev.* **8** e1513

Supper R, Ottowitz D, Jochum B, Kim J H, Römer A, Baron I, Pfeiler S, Lovisolo M, Gruber S and Vecchiotti F 2014 Geoelectrical monitoring: an innovative method to supplement landslide surveillance and early warning *Near Surf. Geophys.* **12** 133–50

Thirugnanam H, Uhlemann S, Reghunadh R, Ramesh M V and Rangan V P 2022 Review of landslide monitoring techniques with IoT integration opportunities *IEEE J. Sel. Top. Appl. Earth Obs. Remote Sens.* **15** 5317–38

Tsai W-N, Chen C-C, Chiang C-W, Chen P-Y, Kuo C-Y, Wang K-L, Lin M-L and Chen R-F 2021 Electrical resistivity tomography (ERT) monitoring for landslides: case study in the lantai area, yilan taiping mountain, northeast taiwan *Front. Earth Sci.* **9** 737271

Uhlemann S, Chambers J, Meldrum P, McClure P and Dafflon B 2021 Geophysical monitoring of landslides–a step closer towards predictive understanding? *Understanding and Reducing Landslide Disaster Risk: Volume 3 Monitoring and Early Warning 5th* pp 85–91

Uhlemann S, Chambers J, Wilkinson P, Maurer H, Merritt A, Meldrum P, Kuras O, Gunn D, Smith A and Dijkstra T 2017 Four-dimensional imaging of moisture dynamics during landslide reactivation *J. Geophys. Res.* **122** 398–418

Uhlemann S, Smith A, Chambers J, Dixon N, Dijkstra T, Haslam E, Meldrum P, Merritt A, Gunn D and Mackay J 2016 Assessment of ground-based monitoring techniques applied to landslide investigations *Geomorphology* **253** 438–51

Watlet A *et al* 2023 4D electrical resistivity to monitor unstable slopes in mountainous tropical regions: an example from Munnar, India *Landslides* **20** 1031–44

Waxman M H and Smits L J M 1968 Electrical conductivities in oil-bearing shaly sands *Soc. Pet. Eng. J.* **8** 107–22

Whiteley J S, Chambers J E, Uhlemann S, Wilkinson P B and Kendall J M 2019 Geophysical monitoring of moisture-induced landslides: a review *Rev. Geophys.* **57** 106–45

Whiteley J S, Watlet A, Kendall J M and Chambers J E 2021a Brief communication: the role of geophysical imaging in local landslide early warning systems *Nat. Hazards Earth Syst. Sci.* **21** 3863–71

Whiteley J S, Watlet A, Uhlemann S, Wilkinson P, Boyd J P, Jordan C, Kendall J M and Chambers J E 2021b Rapid characterisation of landslide heterogeneity using unsupervised classification of electrical resistivity and seismic refraction surveys *Eng. Geol.* **290** 106189

Whiteley J, Inauen C, Wilkinson P, Meldrum P, Swift R, Kuras O and Chambers J 2023 Assessing the risk of slope failure to highway infrastructure using automated time-lapse electrical resistivity tomography monitoring *Transp. Geotech.* **43** 101129

Wicki A and Hauck C 2022 Monitoring critically saturated conditions for shallow landslide occurrence using electrical resistivity tomography *Vadose Zone J.* **21** e20204

Wilkinson P B, Uhlemann S, Chambers J E, Meldrum P I and Loke M H 2015 Development and testing of displacement inversion to track electrode movements on 3-D electrical resistivity tomography monitoring grids *Geophys. J. Int.* **200** 1566–81

Wilkinson P, Chambers J, Uhlemann S, Meldrum P, Smith A, Dixon N and Loke M H 2016 Reconstruction of landslide movements by inversion of 4-D electrical resistivity tomography monitoring data: LANDSLIDE MOVEMENTS FROM ERT INVERSION *Geophys. Res. Lett.* **43** 1166–74

Zakaria M T, Mohd Muztaza N, Zabidi H, Salleh A N, Mahmud N and Rosli F N 2022 Integrated analysis of geophysical approaches for slope failure characterisation *Environ. Earth Sci.* **81** 299